Components of a Highly Integrated DBF Terminal Antenna for Mobile Ka-Band Satellite Communications

Leif C. Stange[1], Holger Pawlak[1], Achim Dreher[2], Sybille Holzwarth[3], Arne F. Jacob[1], Oliver Litschke[3], Michael Thiel[2]

[1] Techn. Universität Braunschweig, Institut für Hochfrequenztechnik, 38023 Braunschweig, Germany
[2] DLR, Institut für Kommunikation und Navigation, 82230 Wessling, Germany
[3] IMST GmbH, 47475 Kamp-Lintfort, Germany

Abstract — **In this paper several components for a highly integrated digital beamforming (DBF) antenna array for Ka-band satellite systems are presented. The general concept of array construction based on a modular approach is introduced and the construction of a constituent array module discussed. Following this outline, different components, designed and tested to later be incorporated into the array module, are treated with the focus set on the Ka-band receiver and transmitter frontends.**

I. Introduction

Mobile broadband data services for internet access over satellite, mainly operating in the Ku-band, will be made available to air passengers by many airlines in the near future. The ever increasing demand for higher bandwidth already promotes the utilization of higher frequency bands. Most projected broadband satellite systems are to operate in the Ka-band, at 20 GHz for downlink and 30 GHz for uplink. The success of these systems will also depend on the availability of user terminals. In contrast to fixed satellite terminals employing large reflector-type antennas, mobile applications will push the demand for smart terminals with digital beamforming (DBF) capabilities. Such terminals allow fast beamscanning, adaptive beamforming, and multiple-beam generation on software basis. For a DBF antenna array these advantages are paid by a higher complexity since each antenna element has to be equipped with dedicated active receiver and/or transmitter circuitry to obtain full digital control of the respective signals.

Depending on the link parameters of targeted satellite systems the total number of antenna elements will amount to 1000 .. 2000. Due to limited fabrication yield it is not reasonable to integrate a complete array of this size monolithically. Thus, for the terminal described herein a modular approach of construction was selected. The basic architecture is sketched in Fig. 1. The antenna array is subdivided into modules, each actually holding 4 x 4 = 16 antenna elements together with the analog receiver/transmitter circuitry up to the analog/digital converters. The module base serves several cross-module functions such as digital signal processing for beamsteering and beamforming, power supply, distribution of local oscillator signals, and thermal management for the array modules.

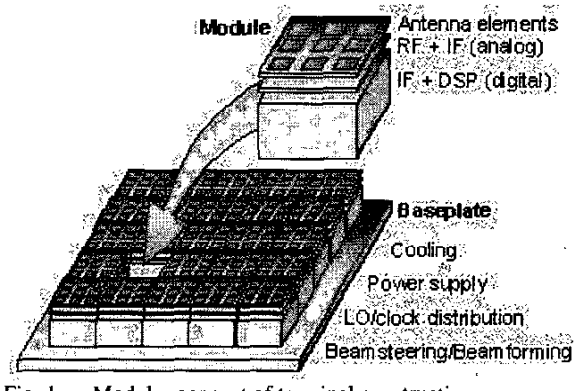

Fig. 1. Modular concept of terminal construction.

The realization of said 16-element array module as a technology demonstrator is the goal of an ongoing project based on an earlier concept study [1]. The objective of this paper is to outline the design of the array module and to present test results of different active and passive components that were developed during the first project phase. The focus is set on the RF frontend part of the module including the antennas, the feed structures, and the Ka-band parts of the electronic circuitry, consisting of commercially available mm-wave monolithic integrated circuits (MMIC).

II. Module Construction

As was already pointed out, a DBF array requires complete receiver and/or transmitter circuits for each antenna element. At Ka-band frequencies this leads to very high integration densities since the inter-element

0-7803-7695-1/03/$17.00 © 2003 IEEE

spacing is dictated by half the wavelength of operation to avoid grating lobes. Hence, the footprint available for a single antenna element and its respective electronic circuit is only (7.5 mm)² for the receiver and (5 mm)² for the transmitter part. This high integration density and associated problems of thermal management constitute one of the reasons to foresee separate receiver and transmitter arrays.

Fig. 2 shows a schematic view of the module construction, common for both the receiver and the transmitter module. The planar antenna elements on the top layer of the module are separated from the electronic circuitry by a metal plate serving as ground plane, structural support, and heat sink/spreader. They are fed through ceramic-filled waveguides inserted into the plate. The MMIC and filter chips constituting the Ka-band frontend circuitry are bonded to the metal ground plate for good electrical and thermal contact.

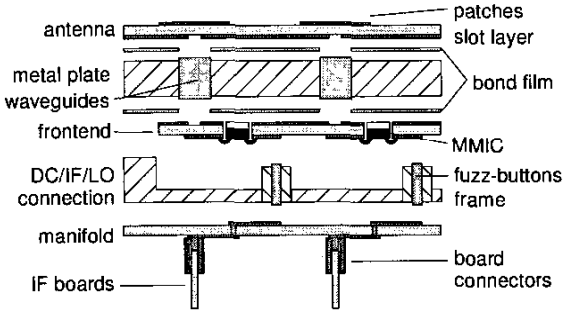

Fig. 2. Schematic construction of the module.

Unlike the RF frontend, the intermediate frequency (IF) parts of the circuitry will have to be integrated using standard printed circuit board (PCB) technology and mounted perpendicularly to the array surface due to the limited integration density achievable with the available components. The interconnection of the RF part and the IF circuitry will be provided by solderless fuzz-button connectors [2] through a distribution manifold, routing the supply, IF, and local oscillator (LO) signals to or from the frontend. The LO signals will be generated by central synthesizers in the module base and distributed to all array elements in order to establish fixed phase relationships between them.

The different module components that have been developed and tested will be discussed in more detail in the next sections. The organization follows the signal path from the antenna elements to the IF circuitry, as outlined above. Additionally the cooling concept and test results for the transmitter will be presented.

III. Antenna Elements and Feeds

For the receiver as well as for the transmitter array microstrip patch radiators were designed, albeit with slightly different approaches. For the receiving part the circular polarization required from the satellite system is realized using linearly polarized square patch elements in a sequentially rotated arrangement [3], yielding circular polarization in the array ensemble. In the transmitter array inherently circularly polarized patches with truncated corners are utilized. These are also arranged in a sequentially rotated way to further enhance the polarization behavior.

The radiators are fed through slots underneath the patches by ceramic-filled circular waveguides drilled into the metal plate that separates the antenna layer from the frontend circuitry. On the circuit side the waveguides are in turn slot-coupled to microstrip lines leading to the active components. This setup is similar to that presented in [4]. The ceramic fill reduces the required waveguide diameter to 3.2 mm ($\varepsilon_r = 11$) and 2.3 mm ($\varepsilon_r = 10$) for the receiver and transmitter, respectively. Besides offering an efficient interconnection through the metal plate, the resonant nature of this setup can be exploited to reduce the filtering needs of the frontend circuitry (cf. Section IV.).

In both designs the antenna substrate as well as the frontend substrate can be fabricated on a single microwave laminate employing standard PCB fabrication processes. They are bonded to the metal plate using selectively applied conductive adhesive or stamped bonding film in order to electrically connect the groundplanes without covering the coupling slots.

To test the technical feasibility of this feeding concept with respect to mechanical and PCB fabrication tolerances, a microstrip-to-waveguide-to-microstrip transition was designed and measured in a back-to-back test setup (2 transitions).

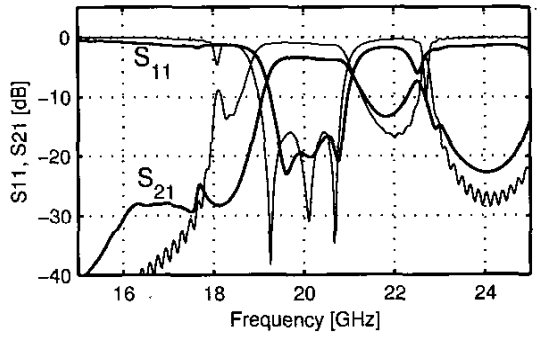

Fig. 3. Microstrip-waveguide transition, simulation (fine line), measurement (bold line).

Fig. 3 shows a comparison between simulation and measurement of the transition for the receiver part. The thickness of the metal plate is 5 mm.

The passband designed from 19 to 21 GHz exhibits a flat response in both simulation and measurement. In the measured data some resonances are frequency-shifted with respect to the simulation, narrowing the passband slightly. The measured insertion loss amounts to about 3.6 dB, corresponding to approx. 1.3 dB per transition (1 dB line losses). A similar test has been conducted for the transmitter feed, showing losses of approx. 1.4 dB per single transition.

IV. RF Frontends

The frontend circuitry of the receiver consists of a low-noise amplifier (LNA) MMIC, an image-reject (IR) filter, and a subharmonically pumped downconverter MMIC with integrated LO amplifier. The transmitter is built up of an upconverter MMIC (again with subharmonic and amplified LO input), an IR-filter, and a medium power amplifier MMIC with moderate current consumption and heat generation. The filter chips, made of gold-plated alumina of 127 µm thickness, are designed and fabricated in-house and can be mounted just like the MMIC.

The MMIC and filters reside in recesses cut into the frontend substrate, a 254 µm thick ceramic loaded Teflon laminate (ε_r = 10.2). The copper conductor traces of this substrate are gold-plated to allow gold-wire bonding for chip interconnection. Molybdenum tabs between the chips and the metal plate are used to match the coefficient of thermal expansion (CTE) of GaAs and to level the chip surface with the substrate surface.

Fig. 4 shows the measured conversion gain of the receiver frontend with IR-filter and the individual contributions to image-rejection by the waveguide feed and the IR-filter over the receive-band frequency.

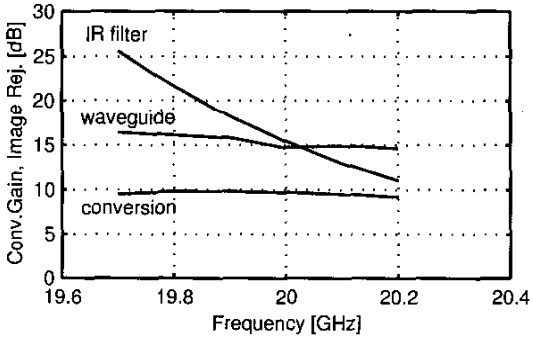

Fig. 4. Receiver frontend conversion gain and image rejection caused by IR filter and waveguide feed, respectively.

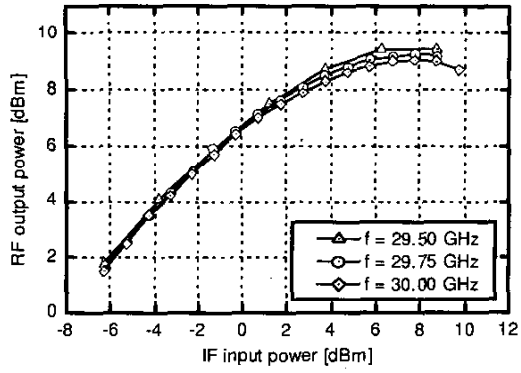

Fig. 5. Transmitter RF output vs. IF input power.

Clearly the feed aids substantially to image-band suppression.

In Fig. 5 the RF output power of the transmitter frontend without IR-filter is diagrammed over the IF input power. For a specified input power level of 0 .. 5 dBm the output power ranges from 6.5 to 9 dBm.

V. Broadband Interconnects

DC supply, IF and LO signals have to be transmitted between the RF frontend and the IF circuitry by vertical connections. Due to the relatively high LO frequencies of approx. 10 and 15 GHz for receiver and transmitter, respectively, this interconnect had to be broadband. Furthermore, the connector was required to be very small in footprint and to allow simple disassembly for repair and rework. The solutions under consideration included metal-on-elastomer (MOE) [5] and fuzz-button connectors [6]. Evaluation of these two concepts showed that basically both can be employed with the fuzz-button transition offering superior performance.

The transitions designed and tested consists of a 50 Ω 3-wire line of fuzz-buttons inserted in a Teflon spacer and compressed between two substrates. The conductor pads on these substrates are arranged in a coplanar (ground-signal-ground) configuration, which is transformed into microstrip line structure using vias, similar to the arrangement used in [5] for MOE transitions.

In Fig. 6 results of a fuzz-button transition between two substrates are shown. Simulation and measurement fundamentally agree. Extending the results presented in [6] it appears that this broadband interconnect is even usable up to frequencies of 20 GHz with insertion losses well below 2 dB. Tests of MOE transitions have shown that insertion losses are below 3 dB at 20 GHz, still significantly better than results presented in [5].

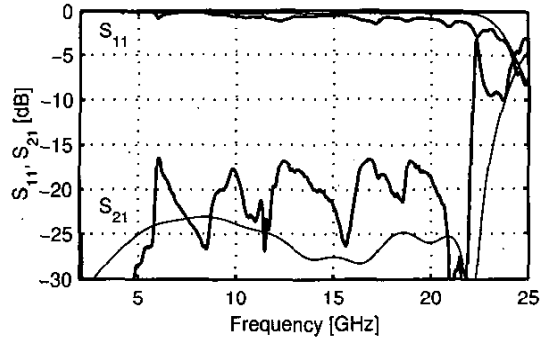

Fig. 6. Fuzz-button transition, simulation (fine line), measurement (bold line).

VI. Cooling Concept

Due to the high integration density heat removal is a critical issue, especially for the transmitter frontend. The heat fluxes occurring are 0.4 W/cm² for the receiver and 2.6 W/cm² for the transmitter. While forced air cooling can be employed for the receiver, the heat generated in the transmitter has to be removed by a liquid cooling system. For this purpose a liquid cooling agent is pumped through a single straight duct buried in the heat spreading metal plate, that separates the antennas and the frontend electronics.

In order to prove the suitability of the concept a thermal test structure was built, shown in Fig. 7. A power resistor was used to generate a realistic heat flux. For simplicity water was chosen as cooling agent. Fig. 8 shows the thermal resistance of the metal plate with single duct. For a moderate flow rate of 80 ml/min a thermal resistance of 1.35 K/W is obtained, corresponding to an excess temperature of 15 K.

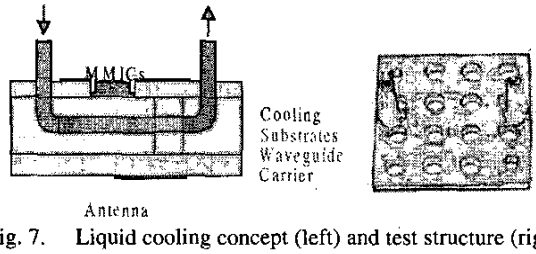

Fig. 7. Liquid cooling concept (left) and test structure (right)

VII. Conclusion

In this paper different components for a DBF antenna array module in Ka-band were presented. These components were developed and tested with the medium-term aim of building a 16-element array module serving as a DBF array technology demonstrator.

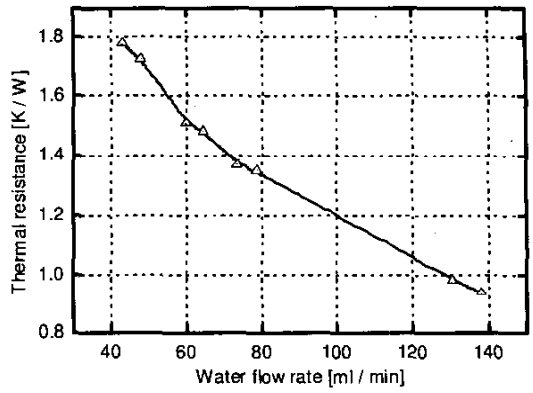

Fig. 8. Thermal resistance of cooled plate vs. water flow rate

The positive test results point at the feasibility of the suggested concept and, thus, can be regarded as an important milestone on the way to the realization of a Ka-band DBF antenna array satellite terminal.

Acknowledgement

The authors wish to acknowledge the funding of this work by the German Ministry of Education and Research (BMBF/DLR) under research contracts 50YB0101 and 50YB0104.

References

[1] A. Dreher, D. Heberling, S. Holzwarth, C. Hunscher, A.F. Jacob, N. Niklasch, H. Pawlak, L. Richard, A. Schroth, L.C. Stange, and M. Thiel, "Ka-band DBF terminal concepts for broadband satellite communications," *25th ESA Antenna Workshop on Satellite Antenna Technology, Noordwijk, The Netherlands*, Sept. 2002, pp. 95-102.

[2] D. Carter, "Fuzz button interconnects at microwave and mm-wave frequencies," *IEE Seminar on Packaging and Interconnects at Microwave and mm-Wave Frequencies*, vol. 3, pp. 1-6, June 2000.

[3] P.S. Hall and M.S. Smith, "Sequentially rotated arrays with reduced sidelobe levels," *Electronic Letters*, vol. 28, no. 18, pp. 1761-1763, August 1992.

[4] P.R. Haddad and D.M. Pozar, "Analysis of two aperture-coupled cavity-backed antennas," *IEEE Trans. Antennas Propagat.*, vol. 45, pp. 1717-1726, December 1997.

[5] F. Colomb, K. Eastman, and J. Roman, "Characterization of metal on elastomer vertical interconnections," *1996 IEEE MTT-S Int. Microwave Symp. Dig.* , vol. 1, pp. 75-77, June 1996.

[6] R. Sturdivant, C. Ly, J. Benson, and M. Hauhe, "Design and performance of a high density 3D microwave module," *1997 IEEE MTT-S Int. Microwave Symp. Dig.*, vol. 2, pp. 501-504, June 1997.